Discovery of Highly Potent p53-MDM2 Antagonists and Structural Basis for Anti-Acute Myeloid Leukemia Activities

Yijun Huang,[†,#] Siglinde Wolf,[‡,#] Barbara Beck,[§,‖,#] Lisa-Maria Köhler,[§] Kareem Khoury,[†] Grzegorz M. Popowicz,[‡] Sayed K Goda,[⊥] Marion Subklewe,[§,‖] Aleksandra Twarda,[¶] Tad A. Holak,[‡,¶] and Alexander Dömling*[†,□]

[†]Department of Pharmaceutical Sciences, School of Pharmacy, University of Pittsburgh, 3501 Fifth Avenue, Pittsburgh, Pennsylvania 15261, United States

[‡]Max Plank Institute for Biochemistry, Am Klopferspitz 18, 82152 Martinsried, Germany

[§]Clinical Cooperation Group Immunotherapy, Helmholtz Zentrum München, Marchioninistrasse 25, 81377 München, Germany

[‖]Department of Internal Medicine III, University of Munich, Campus Großhadern, Marchininistrasse 15, 81377 München, Germany

[⊥]Protein Engineering Unit, Anti-Doping Laboratory-Qatar, Doha, Qatar

[¶]Faculty of Chemistry, Jagiellonian University, Ingardena 3, 30-060 Cracow, Poland

[□]Department for Drug Design, University of Groningen, A. Deusinglaan 1, 9713 AV Groningen, The Netherlands

Ⓢ Supporting Information

ABSTRACT: The inhibition of p53-MDM2 interaction is a promising new approach to non-genotoxic cancer treatment. A potential application for drugs blocking the p53-MDM2 interaction is acute myeloid leukemia (AML) due to the occurrence of wild type p53 (wt p53) in the majority of patients. Although there are very promising preclinical results of several p53-MDM2 antagonists in early development, none of the compounds have yet proven the utility as a next generation anticancer agent. Herein we report the design, synthesis and optimization of YH239-EE (ethyl ester of the free carboxylic acid compound YH239), a potent p53-MDM2 antagonizing and apoptosis-inducing agent characterized by a number of leukemia cell lines as well as patient-derived AML blast samples. The structural basis of the interaction between MDM2 (the p53 receptor) and YH239 is elucidated by a co-crystal structure. YH239-EE acts as a prodrug and is the most potent compound that induces apoptosis in AML cells and patient samples. The observed superior activity compared to reference compounds provides the preclinical basis for further investigation and progression of YH239-EE.
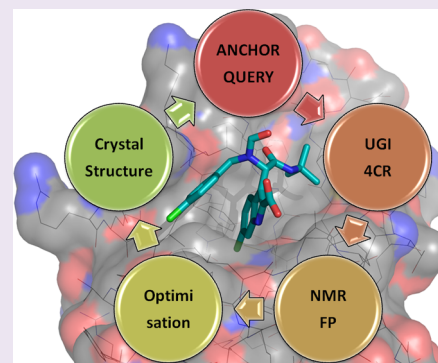
Acute myeloid leukemia (AML) is a malignancy of the hematopoietic system with a poor prognosis, despite the urgent need to develop effective treatments. Up to now 60−70% of AML patients reach a complete remission with a long-term survival of only 25−40%. The protein−protein interaction (PPI) of the transcription factor p53 and its negative regulator MDM2 has emerged as a novel non-genotoxic target for anticancer drugs, and AML seems to be an appropriate disease to test this new approach due to the presence of wild type p53 and overexpression of MDM2 in the majority of AML cases.[1−4] Over 90% of AML patients show no depletion or mutation of p53 but are diagnosed with an up-regulated level of MDM2. Currently the effects of p53-MDM2 antagonists are under investigation, and p53 stabilization and final maturation of AML blast could be shown.[5] A subgroup of AML patients with Flt3-ITD mutation, belonging to the unfavorable risk group with a high risk for relapse, responded more sensitively to p53-MDM2 antagonists.[6]

Although there are several p53-MDM2 antagonists in preclinical and early clinical development, there is no such compound approved for AML treatment to date. The most advanced compound RG7112 (a member of the Nutlin family in the early phase clinical trials) is facing challenges of pharmacokinetic/pharmacodynamic and efficacy and is administered in rather high doses to the patients.[7] Therefore, there is a continuing need for novel approaches in the design of more potent and selective p53-MDM2 antagonists with better efficacy and fewer drawbacks. Based on our recent discovery of a new scaffold class by *in vitro* protein-based optimization, it was surprisingly found that YH239-EE (the ethyl ester prodrug of YH239) exhibits potent anti-AML activity in different cell lines and patient samples.[8] In this contribution, a comprehensive study including discovery by computational chemistry,
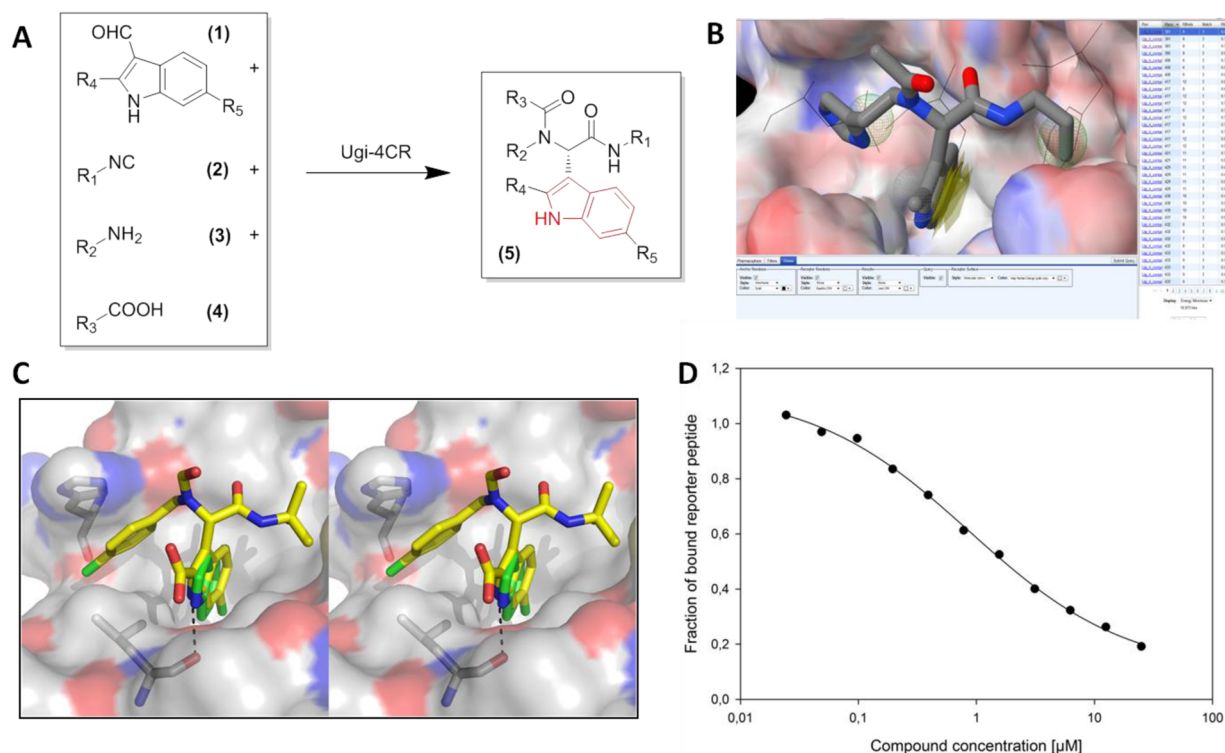
Figure 1. (A) Convergent Ugi-4CR for the rapid synthesis of indole-derived MDM2 antagonists. The anchoring residue is indicated in red. (B) Screenshot of a high ranking Ugi scaffold hit of the ANCHOR.QUERY software. (C) Stereo picture of the co-crystal structure of (S)-YH239 (yellow sticks) in MDM2 (gray, blue, and red surface with the amino acids His96 and Leu54 shown as sticks, PDB ID: 3TJ2). For comparison, the indole ring of Trp23 from the p53-MDM2 complex (PDB ID: 1YCR) is aligned and shown in green sticks. The hydrogen bond between the indole fragment and the carbonyl of Leu54 is indicated by a black dotted line ($d = 2.95$ Å). (D) FP assay of YH239. The normalized value of "fraction of reporter peptide bound" is reported on the y-axis instead of the usual raw mP values due to the fact that the raw mP value fluctuates slightly from experiment to experiment due to changing the active protein concentration and hardware issues. The FP experiments are run in triplicates, and the accuracy errors are ±10%.
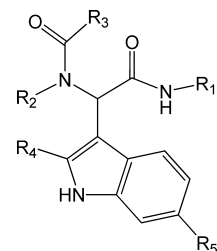
chemical optimization, biochemical, NMR, and X-ray crystallography and cellular characterization in cell lines and patient derived samples is presented to better understand the basis of its anti-AML activity.
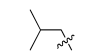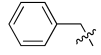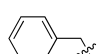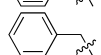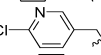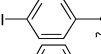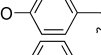
■ RESULTS AND DISCUSSION

Discovery of the α-Aminoacylamide Scaffold of p53-MDM2 Antagonists. We have recently introduced a new technology aiming to enable large-scale design, synthesis, and efficient validation of small molecule protein−protein antagonists.[9] This pharmacophore-based interactive screening technology builds on the role of anchor residues, or deeply buried hot spots contained in the interface of PPIs. These anchors are incorporated into a virtual library of compounds based on various multicomponent reactions (MCRs), delivering tens of millions of readily synthesizable novel compounds.[10] The so-called ANCHOR.QUERY approach has already delivered several novel scaffolds useful to antagonize the p53-MDM2 interaction, which have been biochemically and structurally characterized in several cases.[8,11] The Trp23 is the most deeply buried and central p53 amino acid of the p53-MDM2 interaction and was consequently selected as the anchor. The importance of this amino acid for the p53-MDM2 interaction is also well documented by mutational studies.[12] Other deeply buried amino acid side chains of the p53 hot spot, Phe19 and Leu26, were selected as hydrophobic pharmacophores. Subsequently a ~1/2 billion conformer library based on ~5 million unique compounds containing the indole anchor were
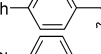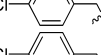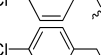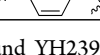
aligned with the Trp23 anchor of p53 and screened for matching the anchor/pharmacophore model.[10] The screening results were then sorted and ranked by molecular descriptors. For example, molecular weight ranking is important for the selection of the compounds to potentially achieve good ligand efficiency. The scaffold and individual compounds are chosen for synthesis according to the binding poses and the electrostatic complementarity in the binding pocket. This method has been validated by several known MCR scaffolds as p53-MDM2 antagonists, including van Leusen 3-CR imidazole, Ugi-5C-4CR iminodicarboxylicacid amide, Ugi-4CR hydantoine, and Orru-3CR imidazolidine.[9,11,13−16] The proposed virtual molecule based on the Ugi four-component reaction (Ugi-4CR)[10] with the lowest molecular weight and matching the pharmacophore points is shown in Figure 1B. This serves as a starting point for validation and optimization in the discovery of new p53-MDM2 antagonists. All molecules based on the α-aminoacylamide scaffold 5 were synthesized using the Ugi-4CR of indolcarbaldehyde 1, isocyanides 2, amines 3, and carboxylic acids 4 as building blocks (Figure 1A).

Affinity-Activity Guided Optimization of p53-MDM2 Antagonists. The scaffold 5 derived from Ugi-4CR was incorporated into the ANCHOR.QUERY screening library due to its great scope and the reliability and compatibility of diverse starting materials.[10,17] For example, 3-formylindole derivatives that serve as anchor building blocks have been previously employed in the Ugi-4CR for the synthesis of alkaloid-like skeletons.[18,19] We used the convergent Ugi-4CR for a fast and

Table 1. Structure–Activity Relationship of Key Compounds to MDM2[a]

ID[1]	R[1]	R[2]	R[3]	R[4]	R[5]	Ki (µM)[2]
5a	benzyl		Me	H	H	n.i.[3]
5b	benzyl		Me	H	H	n.i.[3]
5e'	cyclohexyl		Me	-COOH	Cl	1.6
5i'	cyclohexyl		H	-COOH	Cl	1.6
5o'	*tert*-butyl	Cl	H	-COOH	Cl	4
5p'	*tert*-butyl	Cl	H	-COOH	Cl	10.5
5r'	*tert*-butyl	HO	H	-COOH	Cl	11
5s'	*tert*-butyl	Ph	H	-COOH	Cl	2.5
(±)5l'	*tert*-butyl	Cl	H	-COOH	Cl	0.4
(+)5l'	*tert*-butyl	Cl	H	-COOH	Cl	0.3
(-)5l'	*tert*-butyl	Cl	H	-COOH	Cl	0.7

[a]At the top, the core structure is presented. Compound YH239 is 5l', with -Cl as substituent R[5]. Notes: [1]The numbering corresponds to the Supporting Information. [2]Accuracy of the measurements ±10%. [3]n.i. = no interaction (>60 µM).

efficient elucidation of the structure−activity relationship (SAR) of the α-aminoacylamide scaffold by systematically varying the different starting materials of the Ugi-4CR (Figure 1A, Supporting Information Note 1).

A fluorescence polarization (FP) assay was used to measure the inhibitory affinities of small molecules against the MDM2-p53 complex as previously described by us (Supporting Information Table S1). We measured Nutlin-3a as a reference compound, obtaining K_i = 0.04 µM, which is in excellent agreement with the previously reported value.[20] Additionally NMR, a physically independent method, was used to unambiguously validate the potency of our p53-MDM2 antagonists. We followed a standard protocol for checking the binding of ligands to the target MDM2 protein: a multiple-step titration of a ^{15}N-labeled MDM2 with a compound, monitored with 2D [1]H−[15]N heteronuclear single quantum coherence (HSQC) spectra (cf. Supporting Information Figure S6). The method relies on the use of chemical shift perturbations in 2D [1]H−^{15}N HSQC spectra of ^{15}N-labeled proteins upon addition of ligands or peptides/proteins and works best for proteins of small size (i.e., less than 20 kDa).[21,22] The "binary-titration" was followed by an NMR-based assay developed by us for studying the effect of antagonists on protein−protein interactions (cf. Supporting Information Note 2).[23,24] This NMR assay, named AIDA-NMR (antagonist induced dissociation assay-NMR), belongs to the target protein-detected NMR screening methods and provides unambiguous information on whether an antagonist of a

protein−protein interaction is strong enough to dissociate the complex and whether its action is through denaturation, precipitation, or release of a protein in its functional folded state.[23,24] For effective antagonists, AIDA can also quantitatively characterize antagonist−protein and antagonist−protein−protein interactions in the form of K_D's and fractions of the released proteins from their mutual binding. AIDA requires a large protein fragment (larger than 30 kDa; in the current case, the p53 protein) to bind to a small protein (less than 20 kDa, here the N-terminal domain of MDM2 of ca. 120 amino acids). The FP data in agreement with AIDA and HSQC assays resulted in a reliable, efficient screening for the lead compounds for MDM2 binding.

Key compounds during the SAR evolution are shown in Table 1. The SAR can be summarized as follow. The binding is tolerant with the hydrophobic fragment introduced by several isocyanides (R[1]: benzyl, cyclohexyl, *tert*-butyl), which is designed to occupy the Phe19 pocket of MDM2. However, it turns out that the binding is more sensitive to the hydrophobic fragment introduced by the amine (R[2]), which is designed to occupy the Leu26 pocket of MDM2. As a general trend, it was found that compounds with the free carboxylic acid on R[4] are more potent than the corresponding ethyl ester precursor. Consistent with this finding, we previously showed for an imidazole scaffold that the carboxylic acid group of the indole fragment contributes to the binding by forming water-mediated hydrogen bond contacts to the receptor (PDB IDs: 3LBK and 4DIJ).[25] Moreover this is in accordance with most of the active

compounds/scaffolds that have been co-crystallized in MDM2 in the past, including benzodiazepine (PDB 1T4E), spiroox-indoles (PDV ID: 4JVR), oxopiperidine (PDV ID: 4ERF), nutlin (PDV ID: 4IPF), and others. All of these structures show hydrophilic polar structures at the same position as our -COOH group: benzodiazepine (diazepine carbonyl), spiroox-indoles (oxindole), imidazoles (-COOH), oxopiperidine (-OH), nutlin (urea-carbonyl). Compounds based on unsubstituted indole were found to be inactive (**5a** and **5b**). The binding was also influenced by the fragment introduced by the acid component (R^3): small substituents (H, Me) were well tolerated; however, the introduction of a longer hydrocarbon resulted in decreased activity (**5h**). Benzyl substituents on R^2 showed good activities; however, the substitution pattern around the benzyl group influenced the affinity strongly. Heteroatom introduction into the benzyl group decreased the affinity (**5o′**). Extension of the benzyl group in para position resulted in less active compounds (**5s′**). In total 60 compounds were synthesized and screened in order to optimize the initial hit for affinity to MDM2 (Supporting Information). Racemic compound YH239 (**5l′**, FP: K_i = 400 nM, AIDA: K_D = 300 nM; Figure 2) was found as the most potent one in this series by the
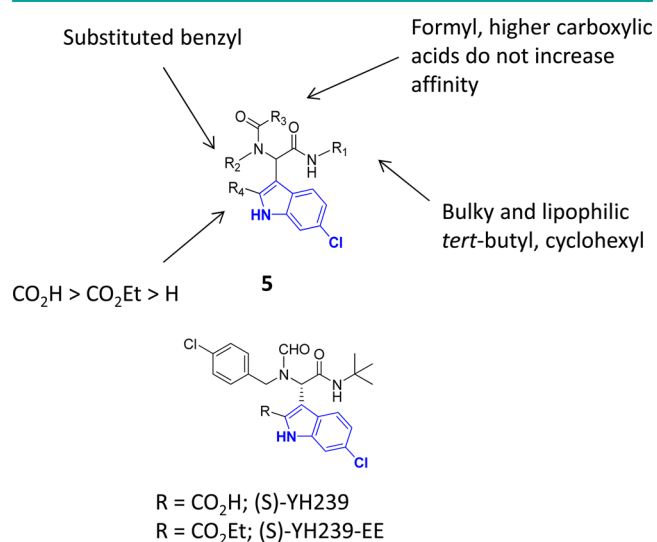

Figure 2. Summarized SAR of scaffold **5** (above) and structures of optimized lead compound YH239 and its ethyl ester YH239-EE (below).

two complementary assays used, which indicates the optimal combination of the fragments (Figure 1D, Supporting Information Figure S6 and Supporting Information Note 2). Interestingly, none of the compounds show significant binding affinity with MDM4 (data not shown), although MDM4 shows significant overall sequence and very close shape similarity to the p53 binding site. Thus YH239 is highly selectively binding to MDM2 over MDM4.

Both enantiomers of the most active compound YH239 were obtained using preparative chiral supercritical fluid chromatography (SFC; Supporting Information Note 3). The enantiomer (+)-YH239 (K_i = 300 nM) is more potent than enantiomer (−)-YH239 (K_i = 700 nM). The "binary titration" experiments, using ^{1}H,^{15}N HSQC, were performed with MDM2, titrated against these two enantiomers. Supporting Information Figure S6 presents the results for (+)-YH239. NMR spectra showed that the (+)-YH239-MDM2 complex was long-lived on the

NMR chemical shift time scale, indicating strong binding with K_D < 1 μM,[22,26,27] as two separate sets of ^{1}H,^{15}N HSQC resonances were observed in the intermediate stages of titration, one corresponding to free MDM2 and the other to the MDM2 bound to the (+)-YH239 compound. The NMR spectra of (−)-YH239-MDM2 titration also showed a slow chemical exchange.

Structural Basis for the Interaction between YH239 and MDM2. The structure−activity study resulted in the optimized compounds with very good binding potency, which encouraged us to co-crystallize a small molecule with the receptor MDM2 in order to better understand the structural basis of the interaction (Table 2). Indeed the enantiomer (S)-

Table 2. Data Collection and Refinement Statistics for the Protein Data Bank (PDB) Accession Code 3TJ2

Data Collection	
space group	P2$_1$
cell constants (Å)	a = 32.44
	b = 58.88
	c = 49.51
	β = 99.208
resolution range (Å)	50−2.1
wavelength (Å)	0.9786
observed reflections	38,681
unique reflections	10,740
whole range	
completeness (%)	98.8
R_{merge}	12.5
$I/\sigma(I)$	8.34
last shell	
resolution range (Å)	2.1 − 2.2
completeness (%)	99.9
R_{merge}	31.6
$I/\sigma(I)$	4.48
Refinement	
no. of reflections	9155
resolution (Å)	19−2.1
R-factor (%)	22.34
R_{free} (%)	30.8
average B (Å^2)	14.4
rmsd bond length (Å)	0.015
rmsd angles (deg)	1.707
Content of Asymmetric Unit	
no. of protein−ligand complexes	2
no. of protein residues/atoms	183/1508
no. of solvent atoms	150

YH239 binds to MDM2 and co-crystallized in the well-established p53-MDM2 binding pocket (Figure 3A).[28] The indole anchor of (S)-YH239 binds in the Trp23 pocket of MDM2. The alignment of the two indoles of (S)-YH239 and Trp23 (rmsd = 0.65 Å) is consistent with the prediction of our modeling approach (Figure 3B). Similar to Trp23 in the p53-MDM2 structure, the indole fragment of (S)-YH239 forms a hydrogen bond to the carbonyl of MDM2's Leu54 (Figure 3C). The benzyl group and the *tert*-butyl group of YH239 mimic Leu26 and Phe19, respectively (Figure 3B). The hydrophobic amino acids make various van der Waals contacts, e.g., the Leu54 methyl group forms short C−H⋯π interaction with the indole fragment (Figure 3C). The *tert*-butyl amide fragment of (S)-YH239 resides in the Phe19 pocket and undergoes plenty
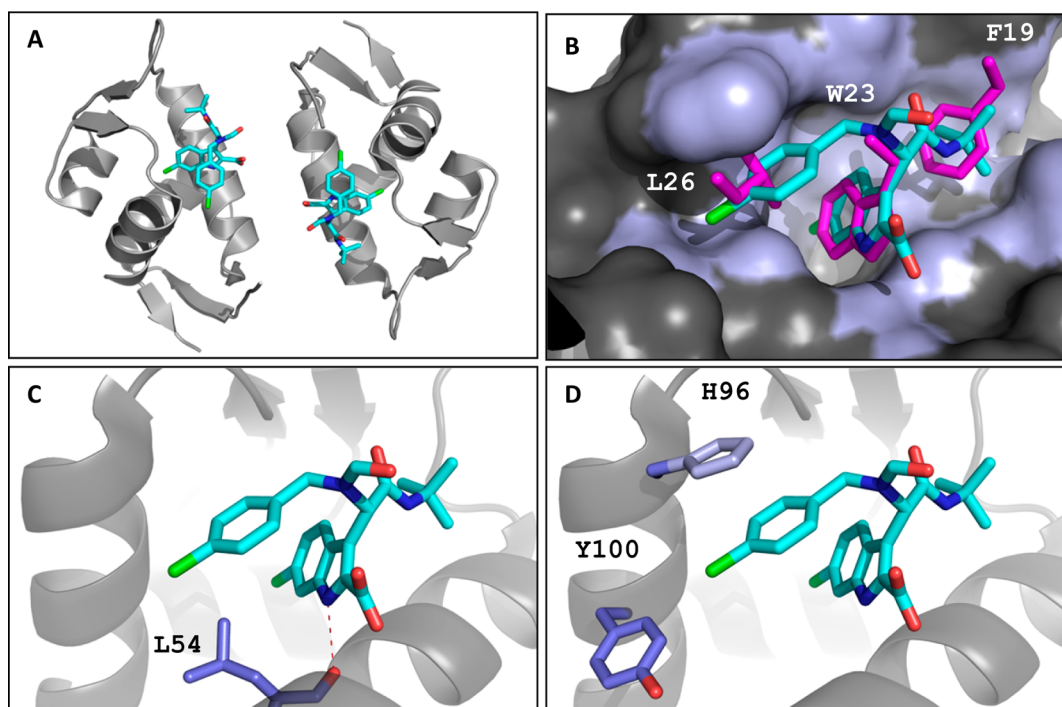
Figure 3. Crystallographic interaction of the MDM2 receptor and (S)-YH239 (cyan sticks). (A) Overall view of the crystallographic MDM2 complex dimer. (B) Alignment of the p53 hot spot triad $F^{19}W^{23}L^{26}$ (magenta sticks, PDB ID: 1YCR) with MDM2-YH239. A 4 Å radius around YH239 is shown as blue surface representation. (C) L54 (blue sticks) undergoes hydrophobic contacts to the 4-chlorobenzyl group and forms a hydrogen bond (red dotted line) to the indole NH (2.9 Å). (D) H96 (blue sticks) is aligning parallel to the benzyl group and forming short contacts (Å). Y100 (blue sticks) is in the characteristic inside-out conformation.

of hydrophobic contacts with the surrounding amino acids, including a short contact to the sulfur of Met62 (2.85 Å, Supporting Information). The 4-chloro benzyl fragment deeply inserts into the Leu26 pocket forming plenty of hydrophobic contacts (Supporting Information). The imidazole ring of His96 at the rim and the phenyl group are aligned parallel and short contacts point to π-stacking interactions (3.1−3.5 Å, Figure 3D). Similar π-stacking contacts with MDM2 are observed in the spirocyclic indolone, the benzodiazepinedione, and the chromenotriazolopyrimidine structures, but not in the imidazole and Nutlin structures.[25,29−31] The two amide groups of (S)-YH239 do not undergo hydrogen bond contacts to the receptor. The formyl group rather points toward the solvent space, indicating that the introduction of solubilizing or affinity-enhancing groups at this position might be useful for further optimization.

YH239-EE Induces Cell Cycle Arrest and Potent Apoptosis of AML Cells. The most potent compounds derived from the biochemical screening and their corresponding ethyl ester precursors were tested in different AML cell lines including various mutational status of p53. The cell lines (OCI-AML-3 and MOLM-13 with wt p53, NB4 with p53 mutation, and HL60 with p53 deletion) were confirmed by p53 sequencing. To get a first impression of the *in vitro* effect of our new p53-MDM2 antagonists, the cells were incubated with 20 μM compound for 72 h evaluating cell proliferation, cell cycle arrest, and induction of apoptosis. The highest ranked compounds from the FP assay and AIDA experiment were first tested for their cellular activity on OCI-AML-3 cells. Surprisingly the most potent antagonist from the biochemical screening, the free carboxylic acid compound YH239, showed no significant effect on the cells with wt p53, but the

corresponding ethyl ester precursor YH239-EE showed potent inhibition of cell proliferation on OCI-AML-3 cells in the same range as Nutlin-3 (Figure 4A). To further investigate the effect of the compounds, we treated four AML cell lines with YH239 and its ethyl ester precursor YH239-EE to observe the induction of cell cycle arrest after 24 h (Figure 4B and C). The accumulation in the sub-G1 phase after treatment with YH239-EE is in all cell lines higher than with YH239. Interestingly YH239 induces MOLM-13 cells in a shift from G2 to M phase, which shows that the compound is transported into the cell.

The induction of apoptosis was determined by treating all four AML cell lines with YH239 and YH239-EE for 72 h and staining with Annexin-V and PI. YH239-EE potently induces apoptosis in AML cell line OCI-AML-3 (YH239 1.3-fold vs YH239-EE 11.8-fold), MOLM-13 (YH239 1.1-fold vs YH239-EE 5.6-fold), and NB4 (YH239 1.2-fold vs YH239-EE 13.1-fold induction of apoptotic cells correlated to untreated control normalized to 1), whereas HL60 cell line shows no apoptotic cells (Figure 4D). A representative example of the response to the free carboxylic acid compound and its corresponding ethyl ester precursor on MOLM-13 cells is shown in Figure 4E. The free carboxylic acid compound YH239 shows almost no apoptotic effect. The number of viable cells in the untreated control (87.6%) after 72 h is similar compared to cells treated by YH239 (92.1%), whereas YH239-EE and Nutlin-3 leads to a high induction of apoptosis.

To determine the IC$_{50}$, the enantiomeric mixture of YH239-EE was separated in the enantiomers (+)-YH239-EE and (−)-YH239-EE by preparative chiral SFC. The MOLM-13 cells were incubated with various concentrations of the compounds and analyzed by measuring the absorbance of formazan.
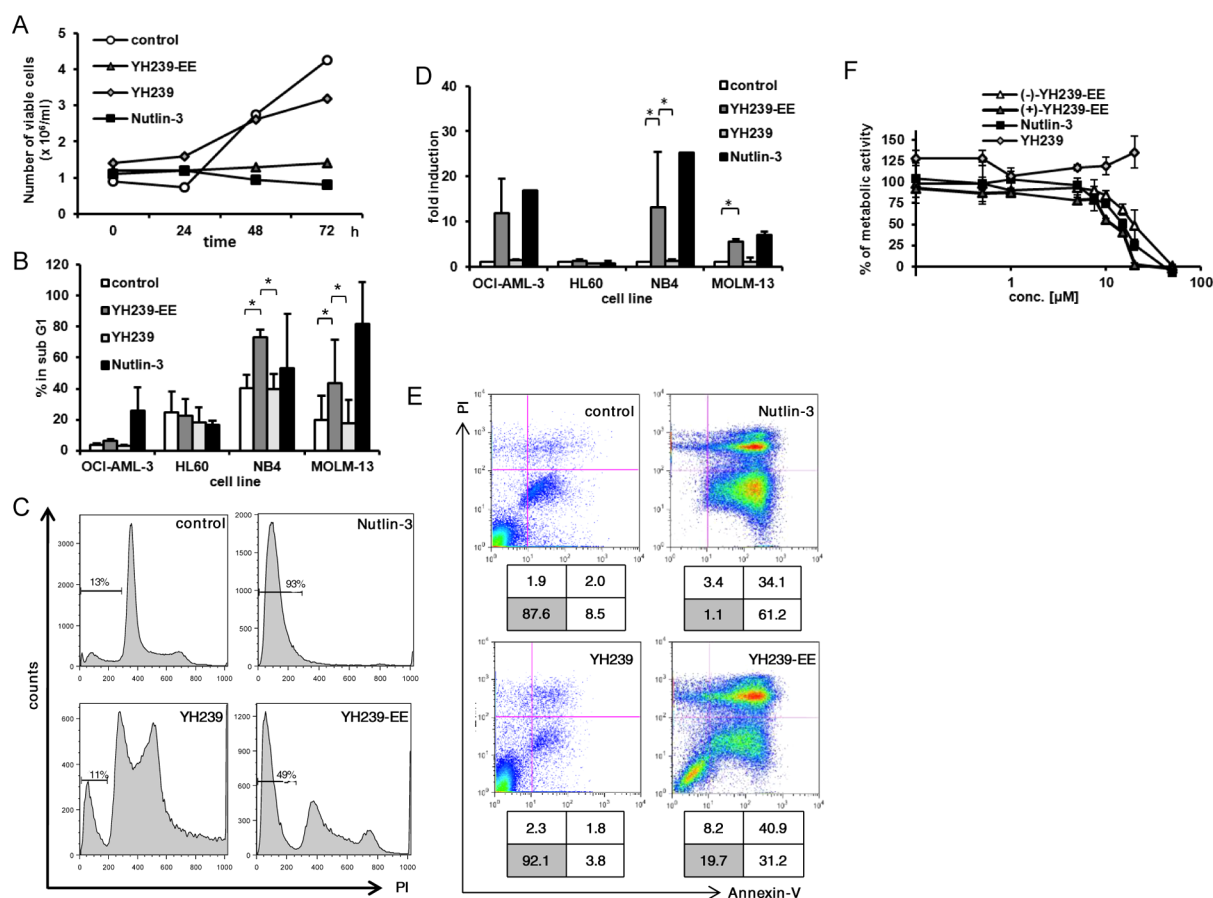
806

dx.doi.org/10.1021/cb400728e | *ACS Chem. Biol.* 2014, 9, 802−811

Figure 4. (A) Biological activity of YH239-EE. YH239-EE inhibits the growth of OCI-AML-3 cells with wild type p53 by inhibiting the p53-MDM2 interaction. Diagram of effects in OCI-AML-3 cell line by Nutlin-3 (black square), YH239 (light gray rhombus), and YH239-EE (dark gray triangle) compared to the untreated control (white circle). The cells were incubated with the substances in a concentration of 20 μM at different time points. The cell viability was determined by staining with Trypan blue. (B) Cell cycle analysis of YH239-EE. The bar chart represents the percentages of the cells in the sub G1 phase in the four different AML cell lines OCI-AML-3 (wild type p53), HL60 (deleted p53), NB4 (mutated p53), and MOLM-13 (wt p53). The cells were treated for 24 h with 20 μM Nutlin-3 (black square), YH239 (light gray square), or YH239-EE (dark gray square) or were left untreated (white square). The cells were fixed in ice-cold ethanol and stained with propidium iodide (PI), and the DNA content was analyzed by flow cytometry. All values are given as means ($n = 3$) with the standard deviations. (C) Cell cycle state of the most sensitive cell line MOLM-13 (wt p53). After treatment with 20 μM Nutlin-3, YH239 and YH239-EE, the cells were fixed, stained with propidium iodide, and treated with RNase. The cells in the subG1 phase were gated. Untreated cells were used as control. (D) Induction of apoptosis in the four different AML cell lines OCI-AML-3 (wt p53), HL60 (deleted p53), NB4 (mutated p53) and MOLM-13 (wt p53). The cells were treated with 20 μM Nutlin-3 (black bar), YH239-EE (dark gray bar), and YH239 (light gray bar) for 72 h. The samples were prepared for Annexin-V and PI staining and analyzed by flow cytometry. The data represent the total of Annexin-V and PI positive/apoptotic and necrotic cells in relation to untreated control set as 1. All values are given as means ($n = 3$) with the standard deviations. (E) Induction of apoptosis in the most sensitive MOLM-13 (wt p53) cells analyzed by flow cytometry. The cells were treated as in panel D. The boxes contain the number of cells belonging to each quadrant in %. (F) The biological activity of the compounds Nutlin-3 (black square), YH239 (light gray rhombus), ($-$)-YH239-EE(white triangle), and (+)-YH239-EE (dark gray triangle) was analyzed by measuring the turnover of WST-1 to formazan depending on the cell metabolism in the MOLM-13 cells after 48 h. All values are given as means ($n = 3$) with the standard deviations.

Corresponding to the data of the FP binding assay, the enantiomer of (+)-YH239-EE showed a higher decrease of metabolic activity with an EC_{50} of 7.5 μM, in contrast to the enantiomer ($-$)-YH239-EE with an EC_{50} of 25.2 μM. The free carboxylic acid compound YH239 showed no effect on MOLM-13 cells (Figure 4F). The separated enantiomers of YH239-EE showed a selectively higher induction of apoptosis after 72 h in one enantiomer ($-$)-YH239-EE (51.5% viable cells) to (+)-YH239-EE (13.7% viable cells). The same effect could be observed in other ethyl ester derivatives from this compound series (data not shown).

YH239-EE Induces p53 and Activates the Apoptotic Caspase 3/7. We further were interested in the target specificity and activation of p53 and downstream targets in the signal transduction pathway of p53. The induction of p53 and MDM2 by (+)-YH239-EE could be shown by Western blot analysis. MOLM-13 (wt-p53) cells were treated with 20 μM (+)-YH239-EE or Nutlin-3 or left untreated for indicated time points and analyzed by Western blot. Comparing to untreated control, an induction of p53 could be observed after 6 h in cells treated by (+)-YH239-EE, whereas MDM2 levels raised after 12 h. As expected from the biochemical screening, no effect on the level of MDM4 could be observed (Figure 5A).

Additionally we investigated our compounds for their capability to induce the caspases 3 and 7 in the apoptotic pathway. The incubation of MOLM-13 cells for various time points with 20 μM (+)-YH239-EE leads to a significant higher
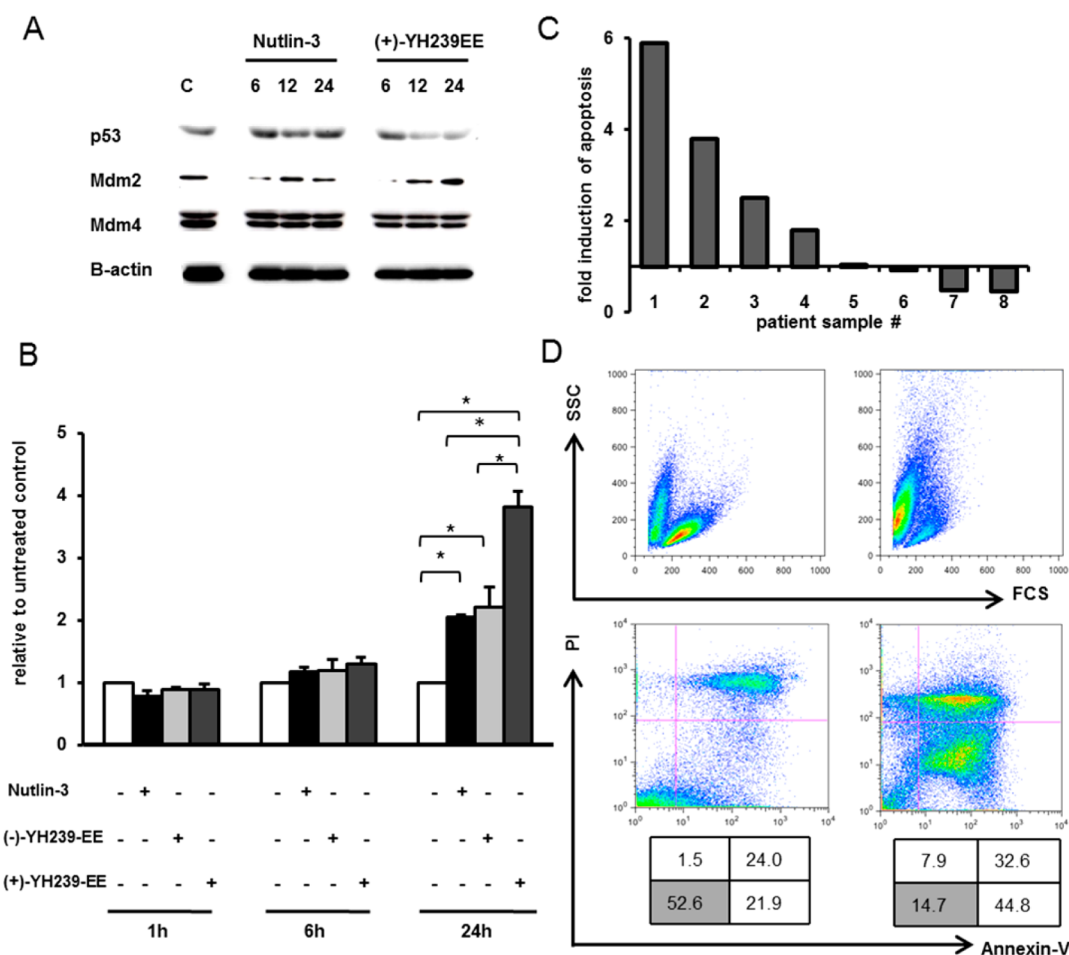
Figure 5. (A) Induction of p53 and downstream target. Western blot analysis of p53, MDM2, and MDM4 on MOLM-13 cells. The cells were treated with 20 μM Nutlin-3 or (+)-YH239-EE or left untreated and were harvested and lysed after 6, 12, and 24 h. The expression of apoptosis-associated proteins was analyzed by Western blot. (B) Induction of the downstream target proteins caspase 3 and 7 in MOLM-13 cells under treatment with Nutlin-3, (−)-YH239-EE, and (+)-YH239-EE. The cells were incubated for 1, 6, and 24 h with a concentration of 20 μM. The caspase activation was assessed with the CaspaseGlo 3/7 assay and is illustrated relative to untreated control set as 1. The bars represent means (n = 3) and standard deviations, *p < 0.05. (C) Induction of apoptosis in AML blasts. The blasts derived from bone marrow or peripheral blood were cultivated on a mouse fibroblast feeder layer, and cell growth was stimulated with an AML cytokine mix. The blasts were treated with (+)-YH239-EE at a concentration of 20 μM. After 72 h the blasts were harvested and stained with Annexin-V, and PI was analyzed by flow cytometry. The bar chart shows the fold induction of apoptosis in primary AML blasts 1−8. The Annexin-V and PI positive blasts were counted and compared with the untreated control set as 1. (D) Exemplary effect of (+)-YH239-EE on patient sample 4 compared to untreated control is shown after treatment for 72 h. The upper row shows the induction of apoptosis in FCS/SSC, and the lower row shows the Annexin-V/PI staining. The boxes contain the number of blasts belonging to each quadrant.

Table 3. Molecular and Cytometric Markers of 8 Primary AML Patient Samples

	AML sample no.							
	1	2	3	4	5	6	7	8
age	43	61	79	49	76	57	70	68
sex[a]	m	f	f	m	f	f	m	m
% AML blasts	83	79	90	70	85	41	45	35
NPM1 mutated	+	+	+	+	−	−	+	−
FLT3-ITD	−	−	+	+	+	−	−	−
karyotype	46,XY [25]	46,XX	48,XY,+4,+8[20]	46,XY [10]	t (3;21)	46,XX	45,XY/46,XY	46,XY

[a] m = male; f = female.

activation of caspase 3 and 7 after 24 h than (−)-YH239-EE and Nutlin-3 (Figure 5B).

Effect of (+)-YH239-EE on Primary Material from AML Patients. We were interested in the effect of the new p53-MDM2 antagonists on primary AML blasts (Table 3). We tested 8 primary patient samples with different mutational

status in NMP1 and Flt-3 and blast level by incubation for 72 h with 20 μM (+)-YH239-EE. The cells were harvested and stained with Annexin-V and PI and were analyzed by flow cytometry. The Annexin-V/PI positive blasts were counted and compared with the untreated control. Under our culture conditions, the untreated AML blasts proliferated and showed

viability in the range of 97.1−52.6% viable cells after 72 h. In 2/3 of the tested samples, we observed an increased induction of apoptosis (Figure 5C and D). Three of the responding AML blasts showed a Flt-3-ITD mutation, and NPM-1 showed an equal distribution over all samples. Interestingly the patient samples with lower blast (<45%) counts showed no response to (+)-YH239-EE. To differentiate the effect between AML blasts and healthy cells, we incubated freshly isolated PBMCs with (+)-YH239-EE and Nutlin-3 for 72 h. In terms of viability, Nutlin-3 showed a higher toxic effect on PBMCs than (+)-YH239-EE (data not shown).

Conclusions. This study disclosed the discovery of YH239, an exquisitely potent p53-MDM2 antagonist, and its prodrug YH239-EE, which can effectively induce apoptosis *in vitro* in different leukemia cell lines as well in several patient derived blasts. The compounds series was designed using a novel pharmacophore-based virtual screening approach, and notably the series could be fast and efficiently optimized using convergent MCR chemistry. FP assay and a complementary NMR-based assay were used to optimize the series for potency. The binding of a potent compound was elucidated by crystallography and was a further great help for the structure-based optimization of the compound series. The binding mode of the small molecule indicates that the three substituents occupy the binding pockets of the p53 hot spot triad FWL, and the compound therefore efficiently competes with the endogenous protein−protein interaction and thus activates wild type p53. YH239 is the most potent p53-MDM2 antagonist described to date (Supporting Information M6) with respect to the ligand efficacy (ΔG/number of heavy atoms) and represents the first structurally characterized acyclic scaffold. The physicochemical properties of YH239 are drug-like (MW: 476 Da, nRB: 7, HBD: 3, HBA: 7, cLogP: 4.2, TPSA: 102). The water solubility of YH239 is good (1.3 mg mL^{-1}, Supporting Information M7), and the compound is chemically accessible in just two steps from simple precursors. The induction of apoptosis in leukemia cell line MOLM-13 was tested for the most potent compounds. However, depending only on protein-based affinity can be misleading during optimization, since crucial ADMET cannot be assessed by this screening. Interestingly the most potent compound in the protein binding assay was YH239 (with a free carboxylic acid), which is *in vitro* less active than its precursor YH239-EE. We therefore speculate that YH239-EE can more effectively enter the cell and is intracellularly activated by a cleavage mechanism resulting in the stronger activity. In addition, we showed that YH239-EE is effectively and in a concentration-dependent manner activating caspase 3 and 7, an early marker of apoptosis. We also tested YH239-EE in 8 different genotyped patient derived blasts. Although the compound showed mixed results ranging from good to no activity, we could show that the compound is specifically inducing apoptosis in AML cancer cells with wt p53 and is less toxic in p53 deleted cell lines. (+)-YH239-EE leads to a higher caspase 3/7 activation and induction of apoptosis than the reference compound Nutlin-3, a derivative of which is currently undergoing early clinical evaluation. Moreover (+)-YH239-EE is less cytotoxic than Nutlin-3. The potent *in vitro* and cell-based activity suggests a potentially therapeutic role of YH239-EE in the treatment of AML.

■ METHODS

Chemistry. Standard chemical techniques were used, and the obtained compounds were analyzed by NMR (Bruker 600 MHz), SFC/HPLC−MS, and biochemical assays. Synthetic, analytical, and SAR details are given in the Supporting Information Note 1 and M8.

Cell Lines and Patient Samples. Four human AML cell lines used in our studies [OCI-AML-3, MOLM-13, HL60, and NB4] were kindly provided from S. Bohlander and K. Spiekermann (Klinikum Großhadern, Munich, Germany) and primarily purchased from DSMZ, Braunschweig, Germany. The authenticity of these cell lines was validated by their mutational status analysis of p53, NMP1, and Flt3-ITD (Laboratory for leukemia diagnostics, Klinikum Großhadern, Munich, Germany and Labor Rost Klein, Munich, Germany). The cell lines OCI-AML-3 and MOLM-13[32] have both wild type p53, HL60[33] deleted and NB4[34] mutated p53. We cultured the cell lines in RPMI 1640 medium (PAN Biotech GmbH) containing 10% heat-inactivated fetal bovine serum (FBS, GIBCO, Invitrogen; LOT 4169705K, REF 10270-106), 0.292 mg mL^{-1} L-Glutamine (GIBCO), 1 M Hepes (GIBCO), 100 units mL^{-1} penicillin (GIBCO) and 100 μg mL^{-1} streptomycin (GIBCO). Cell lines were harvested in log-phase growth and seeded in different concentrations ($1 \times 10^5 - 1 \times 10^6$ mL^{-1}) for the different experiments following exposure to Nutlin-3 (Sigma Aldrich and Nutlin-3a from Cayman Chemical, Ann Arbor, for proliferation assay) and the new p53-MDM2 antagonists (YH compounds). The p53-MDM2 antagonists were used in the concentrations ranging from 50 to 0.1 μM. Heparinized peripheral blood and bone marrow samples were obtained from healthy donors and AML patients after informed consent approved by the Ludwig-Maximilians-Universität, Munich, Germany. Mononuclear cells were isolated by Biocoll Separation Solution (Biochrom) density-gradient centrifugation and cryoconserved. Primary AML mononuclear cells were seeded at 2×10^6 cell mL^{-1} in α-MEM Eagle medium (Pan Biotech) supplemented with a cytokine mix on a MS-5 feeder layer and incubated with p53-MDM2 antagonists for 72 h.[35] In all experiments, cell number and viability were determined by staining cells with Trypan blue 0.4% (Invitrogen) and counted with Countess slides (Invitrogen).

Cell Cycle Analysis. After 24 h of treatment, cells were washed twice with cold PBS (PAN) + 0.1% bovine serum albumin (phosphate buffered saline, pH 7.2, 0.2 μm filtered, Macs BSA stock solution, Milteny Biotec). Then 1×10^6 cells were fixed in ice-cold ethanol (70% v/v) for 1 h, stained with propidium iodide (PI, eBioscence), and treated with RNase (Sigma Aldrich). After 3 h of incubation at 4 °C, the DNA content was determined using the FACS Calibur flow cytometer (Beckton Dickinson Immunocytometry Systems) and analyzed with FlowJo software. The sub-G1 gate standing for non-proliferative cell state was used for determining cell cycle arrest.

Apoptosis Analysis. The apoptosis analysis was performed using the FITC Annexin V Apoptosis Detection Kit I (BD Pharmigen), containing the 10X Annexin Binding Buffer, the FITC Annexin V, and the Propidium Iodide (PI) Staining solution. After incubation with test substances for 72 h, cells were harvested and analyzed. Then 2×10^5 cells were washed twice with ice-cold PBS and resuspended with 1X binding buffer in a concentration of 1×10^6 mL^{-1}. After staining with PI and fluorescein isothiocyanate (FITC)-conjugated Annexin-V (1:20 solution) the cells were incubated for 15 min at RT and then directly analyzed by flow cytometry. Annexin V binds specifically to phosphatidylserine, a lipid that is normally on the inside of the cell membrane but in early apoptosis is exposed on the cell surface. Propidium iodide was used to assess the membrane integrity. The extent of apoptosis induction was then quantified as percentage of Annexin V-positive cells.

WST-1 Cell Proliferation. Cell proliferations were determined by measuring the turnover of WST-1 to Formazan (Roche). Cells were seeded at 5×10^5 mL^{-1} in a 96-well plate and treated with p53-MDM2 antagonists at various concentrations (0.1−50 μM) for the optimized time period of 44 h. The WST-1 reagent was added, and the cells were incubated for additional 4 h. The metabolic activity was determined

photometrically at 440 nm (Sunrise Basic Tecan, Tecan Austria GmbH). IC_{50} values were calculated by Prism (GraphPad Software).

Western Blot Analysis. Treated cells were harvested after various time points, and 1×10^6 cells were solubilized with protein cell lysis buffer. Western blot was performed using the XCell SureLock MINI-Cell (Invitrogen) and the appropriate sample, running, and transfer buffers. Equal amount of protein lysate was loaded into the well of a 12% sodium dodecyl sulfate (SDS)-polyacrylamide gel. After protein separation by electrophoresis (120 V, 60 min), they were transferred to polyvinylidene difluoride (PVDF) membrane (Amersham Hybond-P Membrane, GE Healthcare) by electroblotting (100 V for 2 h). Membranes were blocked, and protein loading was controlled by Ponceau S staining (0.1% Ponceau S (w/v) in 5% (v/v) acetic acid, Sigma Aldrich). The membranes were probed with the following antibodies: mouse monoclonal anti-human p53 protein (Clone DO-7; 1:400 v/v; Dako), rabbit anti-β-actin antibody (1:20000 v/v; Sigma). As secondary antibodies, we used the horseradish peroxidase (HRP) conjugated anti-mouse IgG (1:50000 v/v; Promega) and anti-rabbit IgG (1:50000 v/v; Promega). For detection the membranes were incubated with West Pico chemiluminescent substrate (Thermo Scientific) and signals were detected.

Caspase 3/7 Activation. The caspase activity was measured using the CaspaseGlo 3/7-Assay (Promega). Cells were treated for different time points (1, 6, 24 h) in a 96-well plate with 1×10^4 cells and a volume of 100 μL per well. For analyzing the caspase activity, cells were transferred in a white walled multi-well plate (Brand) and mixed with 100 μL of Caspase Glo Reagent. After incubation time of 1 h the luminescent signal was measured with a luminometer (Wallac Victor^2 1420 multilabel counter, Wallac Cy).

■ ASSOCIATED CONTENT

Ⓢ Supporting Information

Detailed experimental procedures and supplementary figures. This material is available free of charge via the Internet at http://pubs.acs.org.

■ AUTHOR INFORMATION

Corresponding Author
*E-mail: a.s.s.domling@rug.nl.

Author Contributions
#These authors contributed equally to this work.

Notes

The authors declare the following competing financial interest(s): A.D. is inventor of the new compound class and is inventor on the patent owned by the University of Pittsburgh; A.D. is founder of several biotech companies; T.A.H. is founder of Rayaxon GmbH.

■ ACKNOWLEDGMENTS

■ REFERENCES

(1) Wang, S., Zhao, Y., Bernard, D., Aguilar, A., and Kumar, S. (2009) Targeting the MDM2-p53 protein-protein interaction for new cancer therapeutics, in *Protein-Protein Interactions* (Wendt, M. D., Ed.) Vol. 8, pp 57−79, Springer, Berlin, Heidelberg.

(2) Bueso-Ramos, C. E., Yang, Y., deLeon, E., McCown, P., Stass, S. A., and Albitar, M. (1993) The human MDM-2 oncogene is overexpressed in leukemias. *Blood 82*, 2617−2623.

(3) Joerger, A. C., and Fersht, A. R. (2008) Structural biology of the tumor suppressor p53. *Annu. Rev. Biochem. 77*, 557−582.

(4) Joerger, A. C., and Fersht, A. R. (2010) The tumor suppressor p53: from structures to drug discovery. *Cold Spring Harb. Perspect. Biol 2*, a000919.

(5) Secchiero, P., Zerbinati, C., Melloni, E., Milani, D., Campioni, D., Fadda, R., Tiribelli, M., and Zauli, G. (2007) The MDM-2 antagonist nutlin-3 promotes the maturation of acute myeloid leukemic blasts. *Neoplasia 9*, 853−861.

(6) Long, J., Parkin, B., Ouillette, P., Bixby, D., Shedden, K., Erba, H., Wang, S., and Malek, S. N. (2010) Multiple distinct molecular mechanisms influence sensitivity and resistance to MDM2 inhibitors in adult acute myelogenous leukemia. *Blood 116*, 71−80.

(7) Beryozkina, A., Nichols, G. L., Reckner, M., Vassilev, L. T., Rueger, R., Jukofsky, L., Middleton, S., Andreeff, M., Padmanabhan, S., Strair, R., Delioukina, M. L., Maslak, P. G., Hillmen, P., Kurzrock, R., Gore, L., Patnaik, A., Maki, R. G., Schwartz, G. K., Wagner, A. J., and Zhi, J. (2011) Pharmacokinetics (PK) and pharmacodynamics (PD) of RG7112, an oral murine double minute 2 (MDM2) antagonist, in patients with leukemias and solid tumors. *J. Clin. Oncol. 29* (15_suppl, ASCO Annual Meeting Abstracts), 3039.

(8) Huang, Y., Wolf, S., Koes, D., Popowicz, G. M., Camacho, C. J., Holak, T. A., and Dömling, A. (2012) Exhaustive fluorine scanning toward potent p53-MDM2 antagonists. *ChemMedChem 7*, 49−52.

(9) Koes, D., Khoury, K., Huang, Y., Wang, W., Bista, M., Popowicz, G. M., Wolf, S., Holak, T. A., Dömling, A., and Camacho, C. J. (2012) Enabling large-scale design, synthesis and validation of small molecule protein-protein antagonists. *PLoS One 7*, e32839.

(10) Dömling, A., and Ugi, I. (2000) Multicomponent reactions with isocyanides. *Angew. Chem., Int. Ed. 39*, 3169−3210.

(11) Czarna, A., Beck, B., Srivastava, S., Popowicz, G. M., Wolf, S., Huang, Y., Bista, M., Holak, T. A., and Dömling, A. (2010) Robust generation of lead compounds for protein−protein interactions by computational and MCR chemistry: p53/HDM2 antagonists. *Angew. Chem., Int. Ed. 49*, 5352−5356.

(12) Picksley, S. M., Vojtesek, B., Sparks, A., and Lane, D. P. (1994) Immunochemical analysis of the interaction of p53 with MDM2 - fine mapping of the MDM2 binding-site on p53 using synthetic peptides. *Oncogene 9*, 2523−2529.

(13) Popowicz, G. M., Dömling, A., and Holak, T. A. (2011) The structure-based design of MDM2/MDMX−p53 inhibitors gets serious. *Angew. Chem., Int. Ed. 50*, 2680−2688.

(14) Popowicz, G. M., Czarna, A., Wolf, S., Wang, K., Wang, W., Dömling, A., and Holak, T. A. (2010) Structures of low molecular weight inhibitors bound to MDMX and MDM2 reveal new approaches for p53-MDMX/MDM2 antagonist drug discovery. *Cell Cycle 9*, 1104−1111.

(15) Srivastava, S., Beck, B., Wang, W., Czarna, A., Holak, T. A., and Dömling, A. (2009) Rapid and efficient hydrophilicity tuning of p53/MDM2 antagonists. *J. Comb. Chem. 11*, 631−639.

(16) Huang, Y., Wolf, S., Bista, M., Meireles, L., Camacho, C., Holak, T. A., and Dömling, A. (2010) 1,4-Thienodiazepine-2,5-diones via MCR (I): synthesis, virtual space and p53-MDM2 activity. *Chem. Biol. Drug Design 76*, 116−129.

(17) Dömling, A., and Huang, Y. J. (2010) Piperazine scaffolds via isocyanide-based multicomponent reactions. *Synthesis 17*, 2859−2883.

(18) Ribelin, T. P., Judd, A. S., Akritopoulou-Zanze, I., Henry, R. F., Cross, J. L., Whittern, D. N., and Djuric, S. W. (2007) Concise construction of novel bridged bicyclic lactams by sequenced Ugi/RCM/Heck reactions. *Org. Lett. 9*, 5119−5122.

(19) Wang, W., Herdtweck, E., and Dömling, A. (2010) Polycyclic indole alkaloid-type compounds by MCR. *Chem. Commun. 46*, 770−772.

(20) Czarna, A., Popowicz, G. M., Pecak, A., Wolf, S., Dubin, G., and Holak, T. A. (2009) High affinity interaction of the p53 peptide-analogue with human MDM2 and MDMX. *Cell Cycle 8*, 1176−1184.

(21) Shuker, S. B., Hajduk, P. J., Meadows, R. P., and Fesik, S. W. (1996) Discovering high-affinity ligands for proteins: SAR by NMR. *Science 274*, 1531−1534.

(22) Stoll, R., Renner, C., Hansen, S., Palme, S., Klein, C., Belling, A., Zeslawski, W., Kamionka, M., Rehm, T., Mühlhahn, P., Schumacher, R., Hesse, F., Kaluza, B., Voelter, W., Engh, R. A., and Holak, T. A. (2001) Chalcone derivatives antagonize interactions between the human oncoprotein MDM2 and p53. *Biochemistry 40*, 336−344.

(23) Krajewski, M., Rothweiler, U., D'Silva, L., Majumdar, S., Klein, C., and Holak, T. A. (2007) An NMR-based antagonist induced dissociation assay for targeting the ligand-protein and protein-protein interactions in competition binding experiments. *J. Med. Chem. 50*, 4382−4387.

(24) Bista, M., Kowalska, K., Janczyk, W., Dömling, A., and Holak, T. A. (2009) Robust NMR screening for lead compounds using tryptophan-containing proteins. *J. Am. Chem. Soc. 131*, 7500−7501.

(25) Popowicz, G. M., Czarna, A., Wolf, S., Wang, K., Wang, W., Dömling, A., and Holak, T. A. (2010) Structures of low molecular weight inhibitors bound to MDMX and MDM2 reveal new approaches for p53-MDMX/MDM2 antagonist drug discovery. *Cell Cycle 9*, 1104−1111.

(26) Wüthrich, K. (1986) *NMR of Proteins and Nucleic Acids*, Wiley, New York.

(27) Rehm, T., Huber, R., and Holak, T. A. (2002) Application of NMR in structural proteomics: screening for proteins amenable to structural analysis. *Structure 10*, 1613−1618.

(28) Kussie, P. H., Gorina, S., Marechal, V., Elenbaas, B., Moreau, J., Levine, A. J., and Pavletich, N. P. (1996) Structure of the MDM2 oncoprotein bound to the p53 tumor suppressor transactivation domain. *Science 274*, 948−953.

(29) Grasberger, B. L., Lu, T., Schubert, C., Parks, D. J., Carver, T. E., Koblish, H. K., Cummings, M. D., LaFrance, L. V., Milkiewicz, K. L., Calvo, R. R., Maguire, D., Lattanze, J., Franks, C. F., Zhao, S., Ramachandren, K., Bylebyl, G. R., Zhang, M., Manthey, C. L., Petrella, E. C., Pantoliano, M. W., Deckman, I. C., Spurlino, J. C., Maroney, A. C., Tomczuk, B. E., Molloy, C. J., and Bone, R. F. (2005) Discovery and cocrystal structure of benzodiazepinedione HDM2 antagonists that activate p53 in cells. *J. Med. Chem. 48*, 909−912.

(30) Allen, J. G., Bourbeau, M. P., Wohlhieter, G. E., Bartberger, M. D., Michelsen, K., Hungate, R., Gadwood, R. C., Gaston, R. D., Evans, B., Mann, L. W., Matison, M. E., Schneider, S., Huang, X., Yu, D., Andrews, P. S., Reichelt, A., Long, A. M., Yakowec, P., Yang, E. Y., Lee, T. A., and Oliner, J. D. (2009) Discovery and optimization of chromenotriazolopyrimidines as potent inhibitors of the mouse double minute 2−tumor protein 53 protein−protein interaction. *J. Med. Chem. 52*, 7044−7053.

(31) Vassilev, L. T., Vu, B. T., Graves, B., Carvajal, D., Podlaski, F., Filipovic, Z., Kong, N., Kammlott, U., Lukacs, C., Klein, C., Fotouhi, N., and Liu, E. A. (2004) In vivo activation of the p53 pathway by small-molecule antagonists of MDM2. *Science 303*, 844−848.

(32) Matsuo, Y., MacLeod, R. A., Uphoff, C. C., Drexler, H. G., Nishizaki, C., Katayama, Y., Kimura, G., Fujii, N., Omoto, E., Harada, M., and Orita, K. (1997) Two acute monocytic leukemia (AML-M5a) cell lines (MOLM-13 and MOLM-14) with interclonal phenotypic heterogeneity showing MLL-AF9 fusion resulting from an occult chromosome insertion, ins(11;9)(q23;p22p23). *Leukemia 11*, 1469−1477.

(33) Wolf, D., and Rotter, V. (1985) Major deletions in the gene encoding the p53 tumor antigen cause lack of p53 expression in HL-60 cells. *Proc. Natl. Acad. Sci. U.S.A. 82*, 790−794.

(34) Fleckenstein, D. S., Uphoff, C. C., Drexler, H. G., and Quentmeier, H. (2002) Detection of p53 gene mutations by single strand conformational polymorphism (SSCP) in human acute myeloid leukemia-derived cell lines. *Leuk. Res. 26*, 207−214.

(35) Van Gosliga, D., Schepers, H., Rizo, A., Van der Kolk, D., Vellenga, E., and Schuringa, J. J. (2007) Establishing long-term cultures with self-renewing acute myeloid leukemia stem/progenitor cells. *Exp. Hematol. 35*, 1538.